Electronic Supplementary Materials

Heterotrimetallic $Ni_2Ln_2Fe_3$ chain complexes based on $[Fe(1-CH_3im)(CN)_5]^{2-}$

Min Zeng,[a] Kong-Qiu Hu,[a] Cai-Ming Liu[b] and Hui-Zhong Kou[a,]*

[a] Chemistry of Department, Tsinghua University, Beijing 100084, P. R. China

[b] Beijing National Laboratory for Molecular Sciences, Center for Molecular Science, Institute of Chemistry, Chinese Academy of Sciences, Beijing 100190, P. R. China.

Materials and Methods

All reagents were purchased from commercial sources and used without further purification.

Physical measurement

Elemental analyses (C, H, and N) were performed on a Cario Erballo elemental analyzer. IR spectra were measured on a WQF-510A Fourier transform infrared spectrometer. PXRD measurements were recorded on a Bruker D8 ADVANCE X-ray diffractometer. The sweeping speed is 10°/min in the range of 5−50°. Single-crystal X-ray data were collected on a Rigaku Saturn724+ (2x2 bin mode) diffractometer. The structures were solved by direct methods and refined with full-matrix least squares on F^2 using the *SHELXTL-2013* program package. Magnetic measurements were recorded on a Quantum Design MPMS-XL5 SQUID magnetometer. The experimental susceptibilities were corrected for diamagnetism of Pascal's constants.

Synthesis of precursor Ni(valpn)

1,3-diamopropane (1.48 g, 20 mmol) and triethylamine (4.04g, 40 mmol) was added into a 100 mL tetrahydrofuran (THF) solution of o-vanillin (6.08 g, 40 mmol) with stirring for 30 minutes. Then, $Ni(NO_3)_2{\cdot}6H_2O$ (5.82 g, 20 mmol) was added into the abovementioned solution. After the stirring was continued for 1 hour, 400 mL deionized water was added to obtain green precipitation. The resulting precipitation was then filtered, washed, and dried to obtain Ni(valpn).

Synthesis of $[Ca(1\text{-}CH_3im)(H_2O)][Fe(CN)_5(1\text{-}CH_3im)]$

1-methyl imidazole ($1\text{-}CH_3im$, 12.5 g, 15mmol) was added into the 250 mL aqueous solution of $Na_3[Fe(CN)_5(NH_3)]{\cdot}3H_2O$ (10 g, 3 mmol) with stirring. The pH of the solution was then adjusted to 7-8 with HCl solution. Then, 7.5 mL H_2O_2 (30%) was added to above solution. 1 hour later, equal volume saturated solution of $CaCl_2$ was added. The resulting solution was then filtered and evaporated to obtain red powders.

Synthesis of complexes 1 and 2

$[Ni(valpn)Gd(DMF)_{2.5}(H_2O)_{0.5}]_2[Fe(1\text{-}CH_3im)(CN)_5]_3{\cdot}4DMF{\cdot}15H_2O$ (**1**)*:*

Ni(valpn) (43.5mg, 0.1mmo) and $Gd(NO_3)_3{\cdot}6H_2O$ (46 mg, 0.1 mmol) was dissolved in 10 mL MeCN, and $[Ca(1\text{-}CH_3im)(H_2O)][Fe(CN)_5(1\text{-}CH_3im)]$ (41 mg, 0.1 mmol) was added into abovementioned solution to obtain a red-brown precipitate. Then, a small amount of DMF solution was added to dissolve the precipitate. The resulting solution was then filtered and evaporated for several weeks to obtain red-brown plate crystals. Yield: 65%. Anal. Calcd (%) for $C_{92}H_{153}Fe_3Gd_2N_{34}Ni_2O_{33}$: C, 38.60; H, 5.39; N, 16.63. Found: C, 39.1; H, 5.2; N, 16.6. IR (cm^{-1}) : ν(C≡N) 2116, 2133.

$[Ni(valpn)Dy(DMF)_{2.5}(H_2O)_{0.5}]_2[Fe(1\text{-}CH_3im)(CN)_5]_3{\cdot}4DMF{\cdot}12H_2O$ (**2**)*:*

The preparation procedure of complex **2** is similar to that for **1**, except using $Dy(NO_3)_3{\cdot}6H_2O$ (45 mg, 0.1 mmol) instead of $Gd(NO_3)_3{\cdot}6H_2O$. Yield: 67%. Anal. Calcd (%) for $C_{92}H_{147}Dy_2Fe_3N_{34}Ni_2O_{30}$: C, 39.19; H, 5.25; N, 16.89. Found: C, 38.9; H, 5.3; N, 16.3. IR (cm^{-1}) ν(C≡N): 2112, 2130.

Table S1. Crystal and structure refinement parameters for complexes **1-2**

	1	**2**
formula	$C_{92}H_{153}Fe_3Gd_2N_{34}Ni_2O_{33}$	$C_{92}H_{147}Dy_2Fe_3N_{34}Ni_2O_{30}$
Fw	2862.94	2817.38
T/K	153.0	153.0
crystal system	Monoclinic	Monoclinic
space group	C2/c	C2/c
a/Å	26.933(3)	26.924(5)
b/Å	13.0976(15)	13.097(3)
c/Å	39.297(5)	39.319(8)
β/°	101.425(2)	100.35(3)
V /Å^3	13588(5)	13639(5)
Z	4	4
ρ_{calcd}/g cm^{-3}	1.400	1.373
μ(MoKa)/ mm^{-1}	1.622	1.736
F(000)	5876	5772
Ref [I >2σ]	11446	13654
GOF	1.180	1.105
R1[I > 2σ(I)][a]	0.0930	0.0664
wR2 (all data)[b]	0.2065	0.1611
CCDC	2058041	2058042

[a] $R1=\sum\|F_o|-|F_c\|/\sum|F_o|$. [b] $wR2=\left\{\sum\left[w\left(F_o{}^2-F_c{}^2\right)^2\right]/\sum\left[w\left(F_o{}^2\right)^2\right]\right\}^{1/2}$

Table S2. Selected bond length (Å) and angles (º) for complexes **1-2**

	1 ($Gd_2Fe_3Ni_2$)	**2** ($Dy_2Fe_3Ni_2$)		**1** ($Gd_2Fe_3Ni_2$)	**2** ($Dy_2Fe_3Ni_2$)
Ln1–O2	2.269(6)	2.258(4)	Ni1–N1	2.111(9)	2.105(5)
Ln1–O1	2.312(6)	2.289(3)	Fe1–C29	1.922(10)	1.925(6)
Ln1–O5	2.334(7)	2.293(4)	Fe1–C26	1.946(11)	1.944(6)
Ln1–O6	2.329(8)	2.312(4)	Fe1–C22	1.935(12)	1.949(6)
Ln1–O1W/O7	2.360(8)	2.306(5)	Fe1–C27	1.946(10)	1.947(5)
Ln1–N5A	2.463(8)	2.456(4)	Fe1–C21	1.958(10)	1.957(6)
Ln1–O4	2.571(6)	2.550(4)	Fe1–N6	1.967(7)	1.979(4)
Ln1–O3	2.612(6)	2.587(4)	Fe2–C47	1.949(17)	1.880(14)
Ni1–N8	2.023(8)	2.028(4)	Fe2–C9	1.935(12)	1.942(7)
Ni1–O2	2.040(6)	2.033(3)	Fe2–C41	1.939(17)	1.898(13)
Ni1–O1	2.039(7)	2.044(4)	Fe2–C31	1.951(17)	1.965(13)
Ni1–N9	2.054(9)	2.049(5)	Fe2–N14	1.95(2)	2.026(11)
Ni1–N10	2.111(9)	2.098(5)	Ln1---Ni1	3.4433(13)	3.4241(10)
Fe1–C21–N3	178.7(9)	178.1(5)	Fe2–C9–N10	174.9(10)	176.3(6)
Fe1–C22–N2	179.5(11)	178.3(5)	Fe2–C31–N13	176(2)	176.3(13)
Fe1–C26–N1	173.0(8)	173.4(4)	Fe2–C41–N16	176(3)	173(2)
Fe1–C27–N5	174.8(9)	175.1(5)	Fe2–C47–N19	177(4)	175(2)
Fe1–C29–N4	177.6(9)	177.9(5)	C27A–N5A–Dy1	164.7(7)	164.7(4)
C26–N1–Ni1	154.9(7)	153.6(4)	C9–N10–Ni1	157.3(9)	156.1(5)
Ni1–O1–Ln1	104.5(3)	104.26(14)	Ni1–O2–Ln1	105.9(3)	105.75(16)

Symmetry code: A –x, 3-y, 1-z

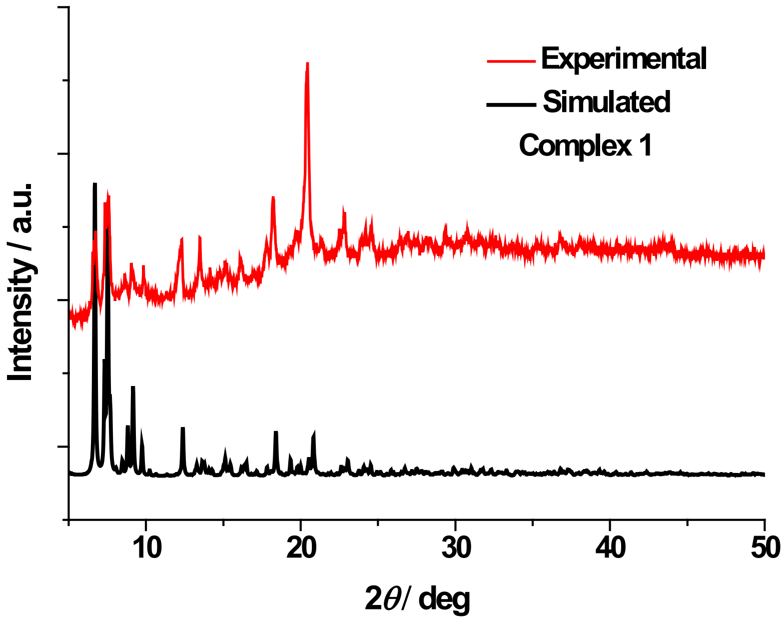

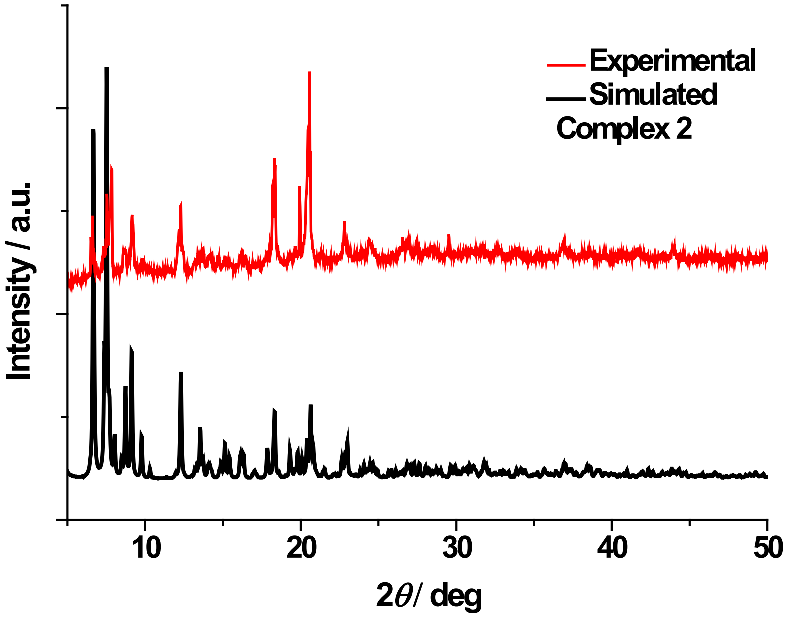

Fig. S1. PXRD patterns for complexes **1** and **2**.

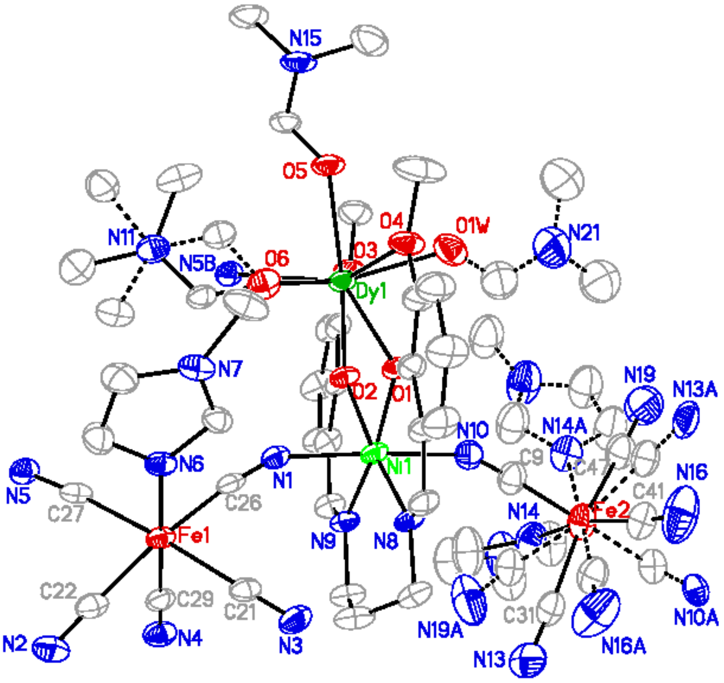

Fig. S2. ORTEP drawing for complex **2** showing 30% probability thermal ellipsoids. The dotted lines represent the disorder.

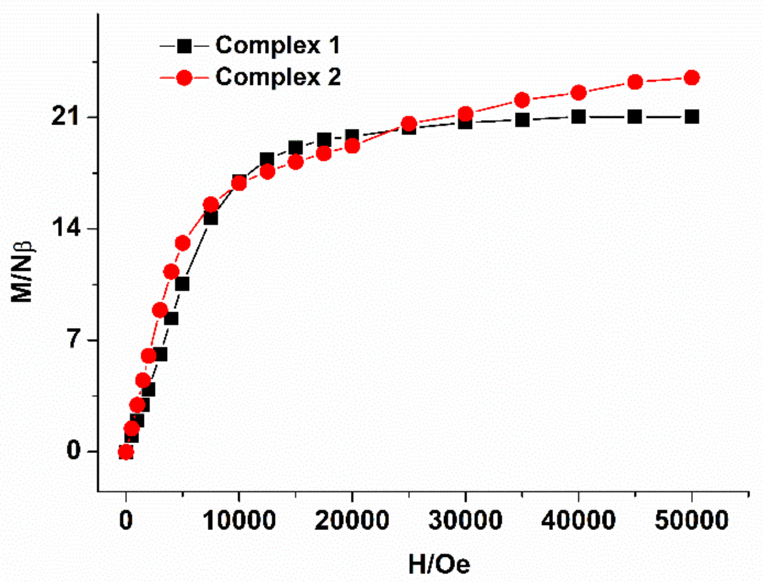

Fig. S3. The M-H curve of complexes **1** and **2** at 2 K.

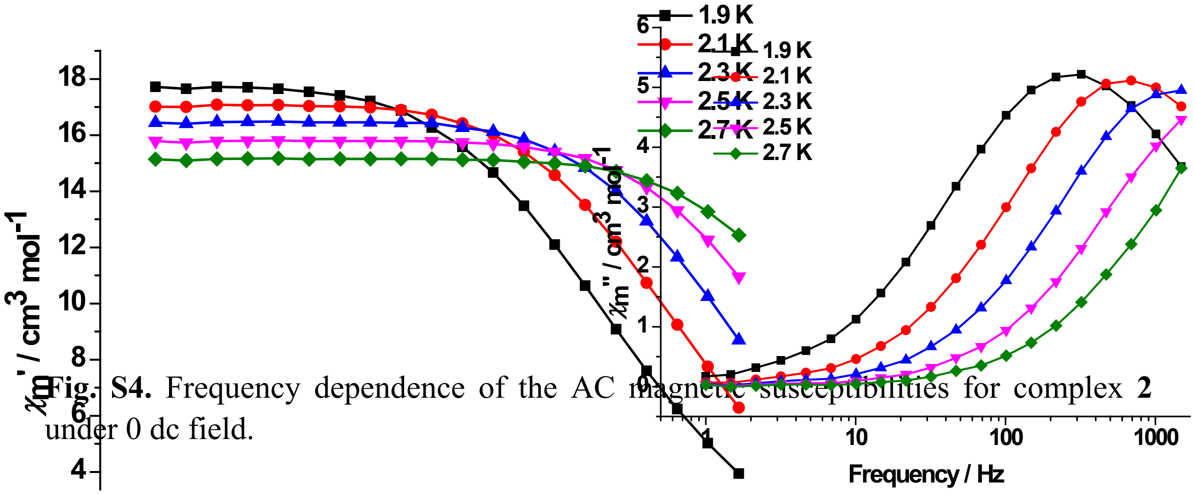

Fig. S4. Frequency dependence of the AC magnetic susceptibilities for complex **2** under 0 dc field.

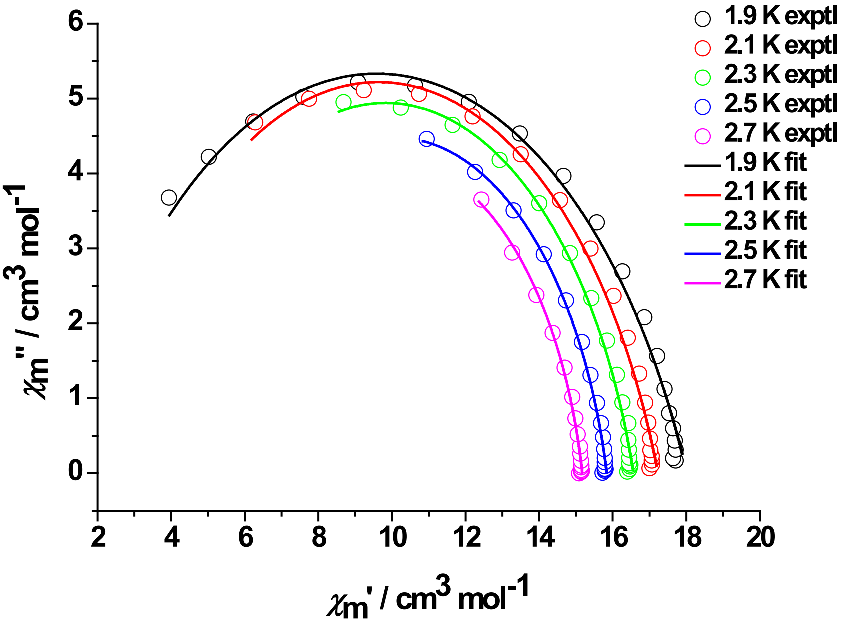

Fig. S5. Cole-Cole plots of complex **2**. The solid lines represent the best fit results.

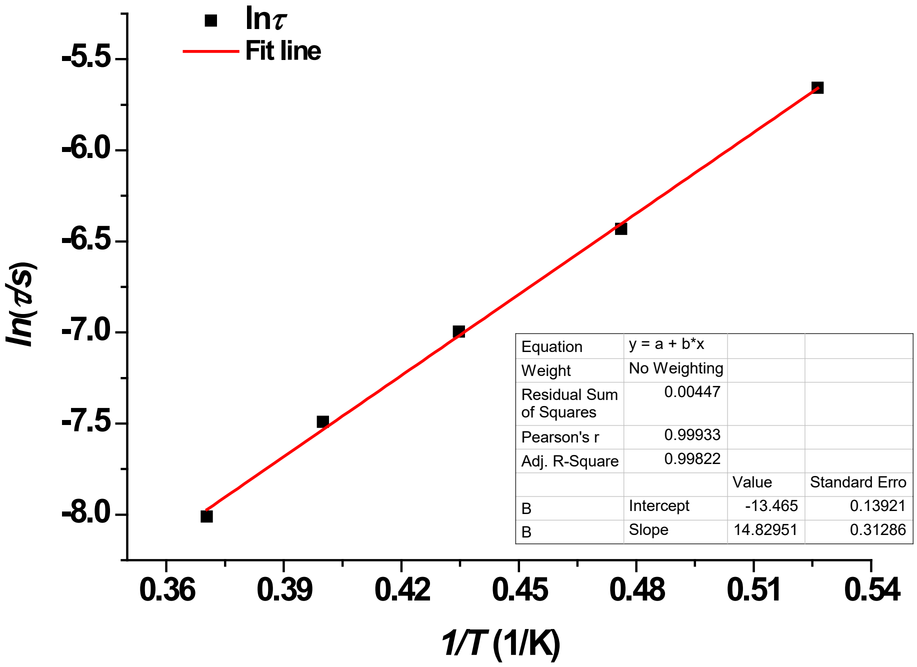

Fig. S6. The ln(τ) vs. T^{-1} plots based on the Arrhenius relationship for complex **2**.

Table S3. Cole-Cole curve fitting parameters for complex **2**.

T / K	α	τ	χ_T	χ_S
1.9	0.282	3.49×10^{-3}	18.019	1.152
2.1	0.234	1.61×10^{-3}	17.232	2.034
2.3	0.194	9.16×10^{-4}	16.566	3.095
2.5	0.155	5.58×10^{-4}	15.840	4.398
2.7	0.137	3.32×10^{-4}	15.174	4.753